Electronic Supplementary Material (ESI) for Journal of Materials Chemistry A.

Supplementary Information

Ultrathin mesoporous NiO nanosheets-anchored 3D nickel foam as advanced electrodes for supercapacitors†

Guanhua Cheng, Wanfeng Yang, Chaoqun Dong, Tianyi Kou, [§] Qingguo Bai, Hao Wang, Zhonghua Zhang *

Key Laboratory for Liquid-Solid Structural Evolution and Processing of Materials (Ministry of Education), School of Materials Science and Engineering, Shandong University, Jingshi Road 17923, Jinan 250061, P.R. China.

[§]*Present address: Department of Chemistry and biochemistry, University of California Santa Cruz, 1156 High Street, Santa Cruz 95064, United States*

**Corresponding author. Email: zh_zhang@sdu.edu.cn; Fax: +86-531-88396978; Tel: +86-531-88396978.*

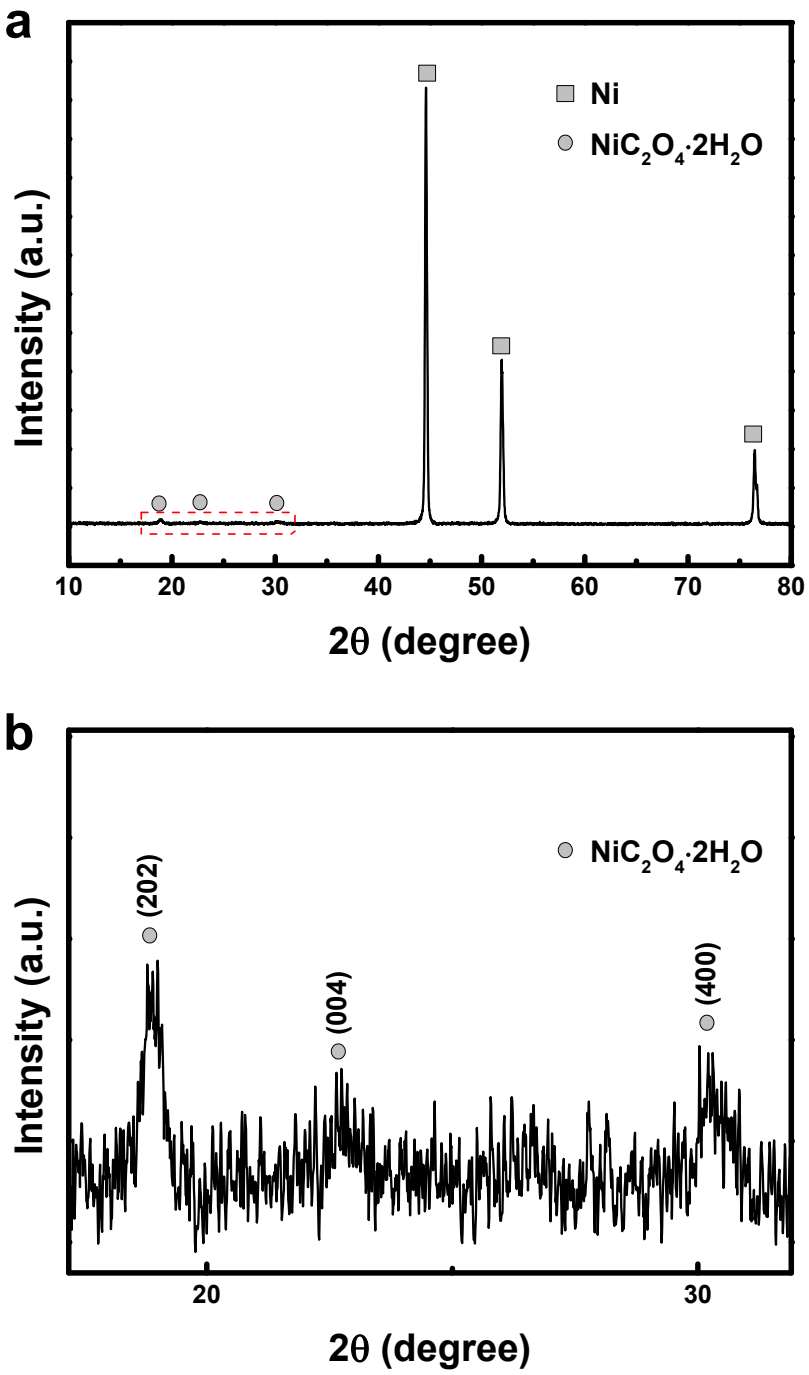

Figure S1. (a) XRD pattern of the nickel foam after immersion in the 0.5 M oxalic acid ethanol solution at 45 ± 2 °C for 0.5 h. (b) The enlarged view of the dash square in (a). The peaks at 2θ=18.6, 22.5, 30.2°are attributed to the reflections of (202), (004), (400) planes of nickel oxalate dihydrate ($NiC_2O_4 \cdot 2H_2O$, PDF #25-0582) respectively, which well confirms the formation of $NiC_2O_4 \cdot 2H_2O$ after immersion.

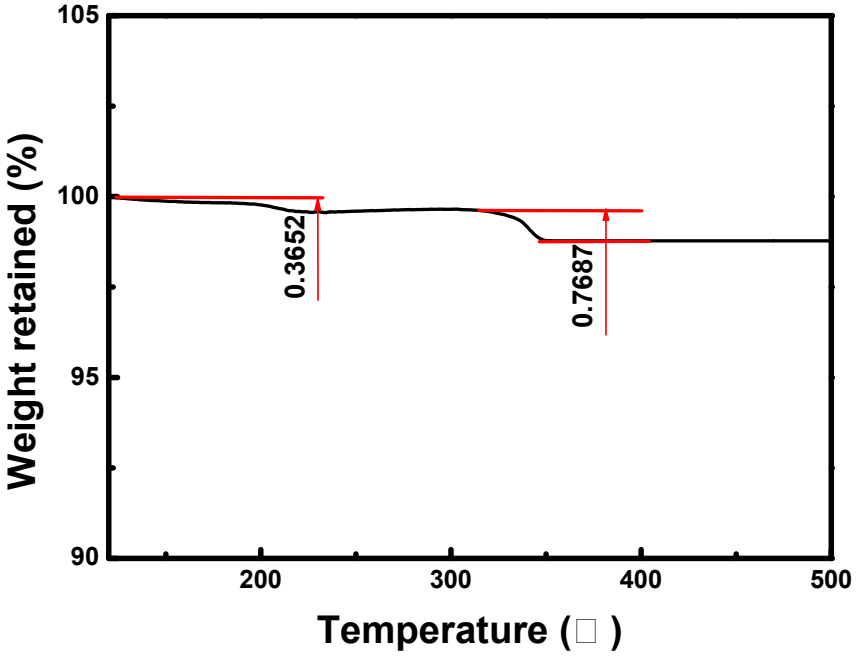

Figure S2. TG curve of the $NiC_2O_4 \cdot 2H_2O$/Ni foam sample.

Figure S3. SEM image of nickel oxalate nanosheets decorated 3D nickel foam at low magnification.

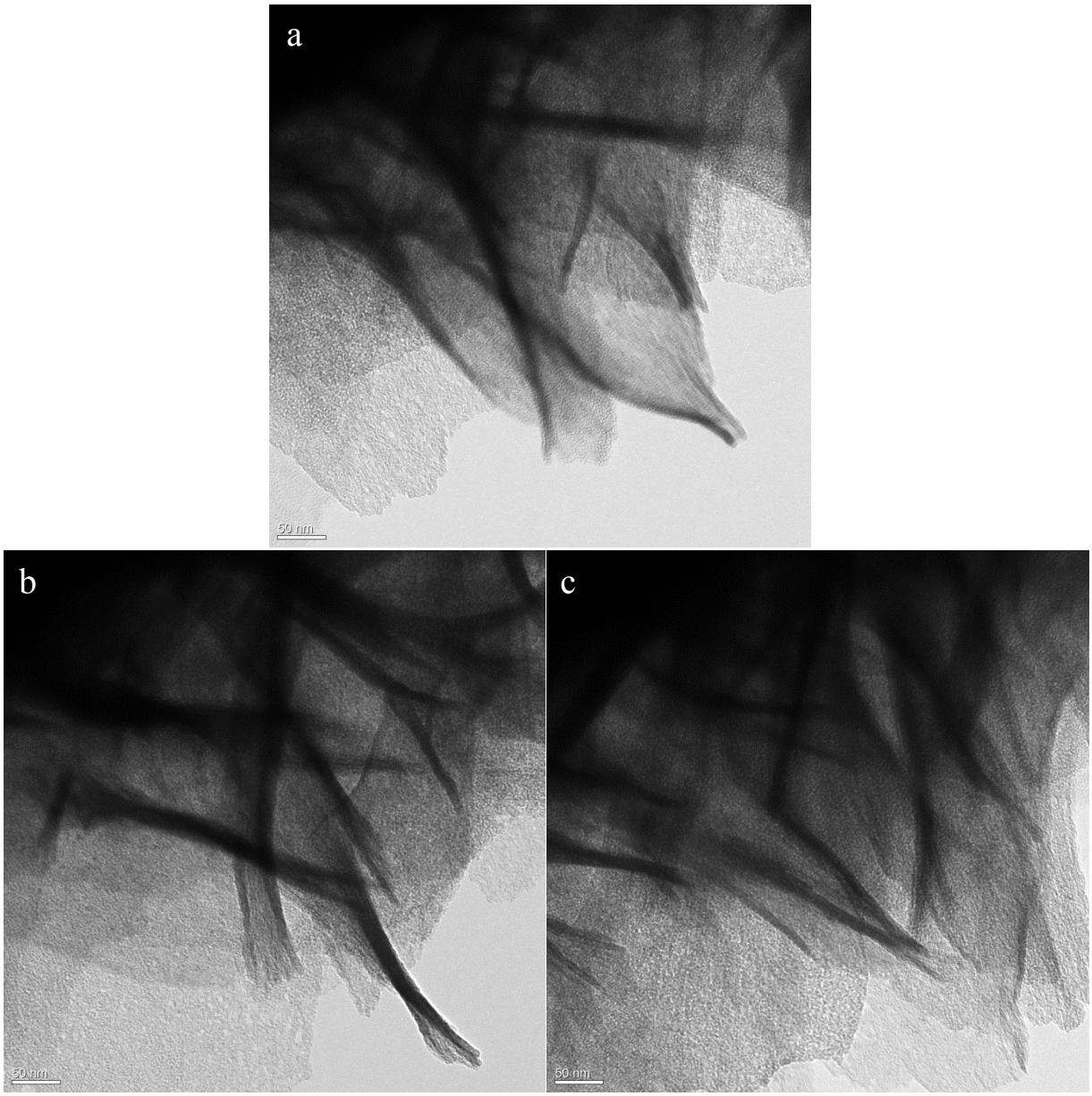

Figure S4. TEM images of the ultrathin mesoporous NiO nanosheets supported on the 3D nickel foam.

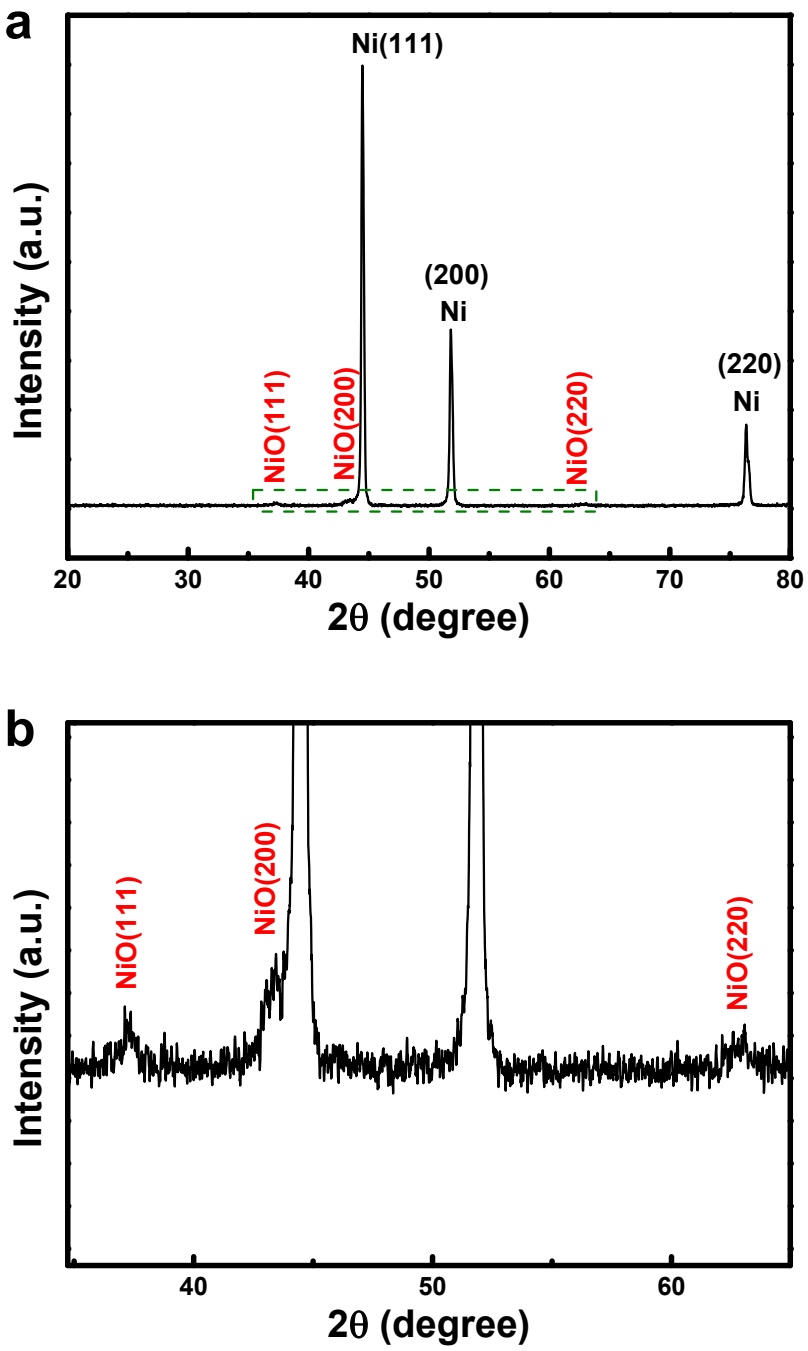

Figure S5. (a)XRD pattern of the ultrathin mesoporous NiO nanosheets supported on the 3D nickel foam. (b) The enlarged view of the dash square in (a).

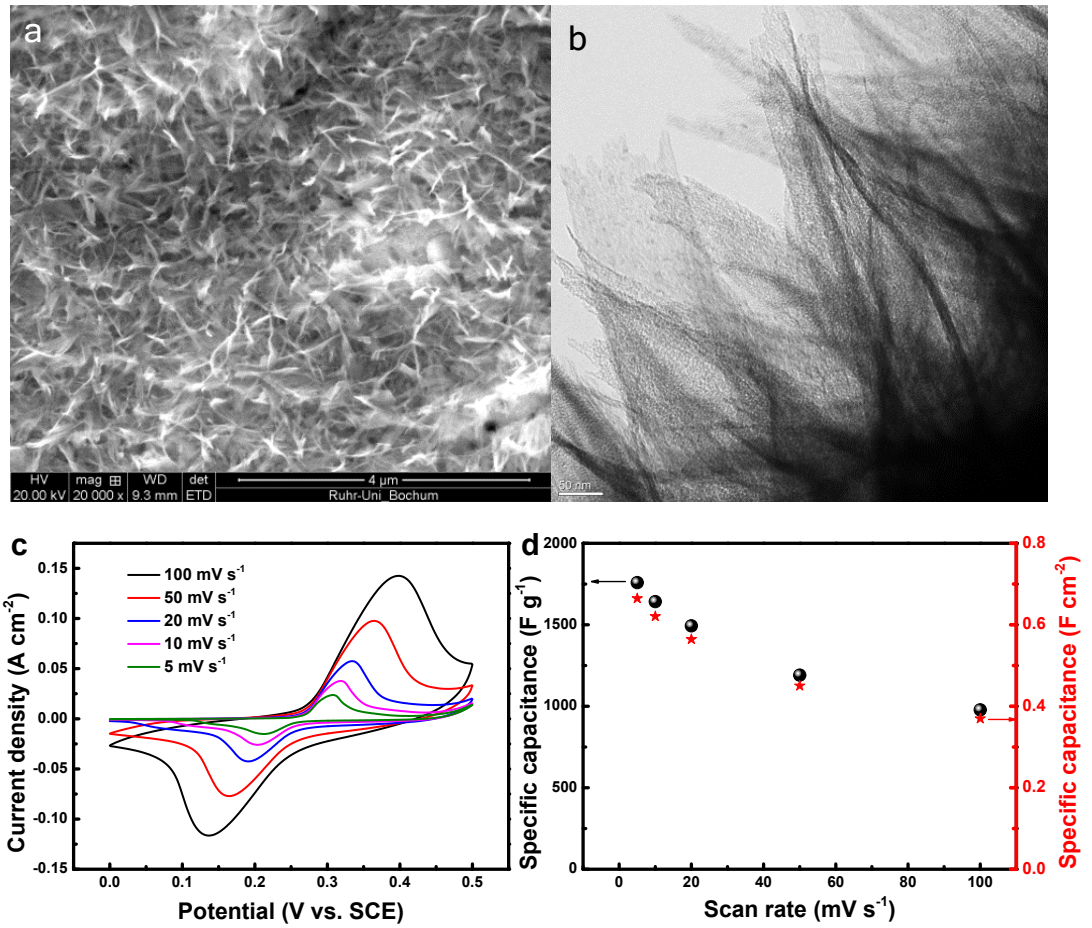

Figure S6. (a) SEM and (b) TEM images of the NiO electrodes with higher loading mass (0.38 ± 0.02 mg cm^{-2}). (c) CV curves of the hybrid electrode measured in the 2 M KOH solution. (d) The mass- and area- normalized specific capacitance as a function of the scan rate. The immersion conditions were as follows: 45± 2 ^{o}C for 1.5 h in the 0.5 M oxalic acid ethanol solution with additional 5 wt.% water.

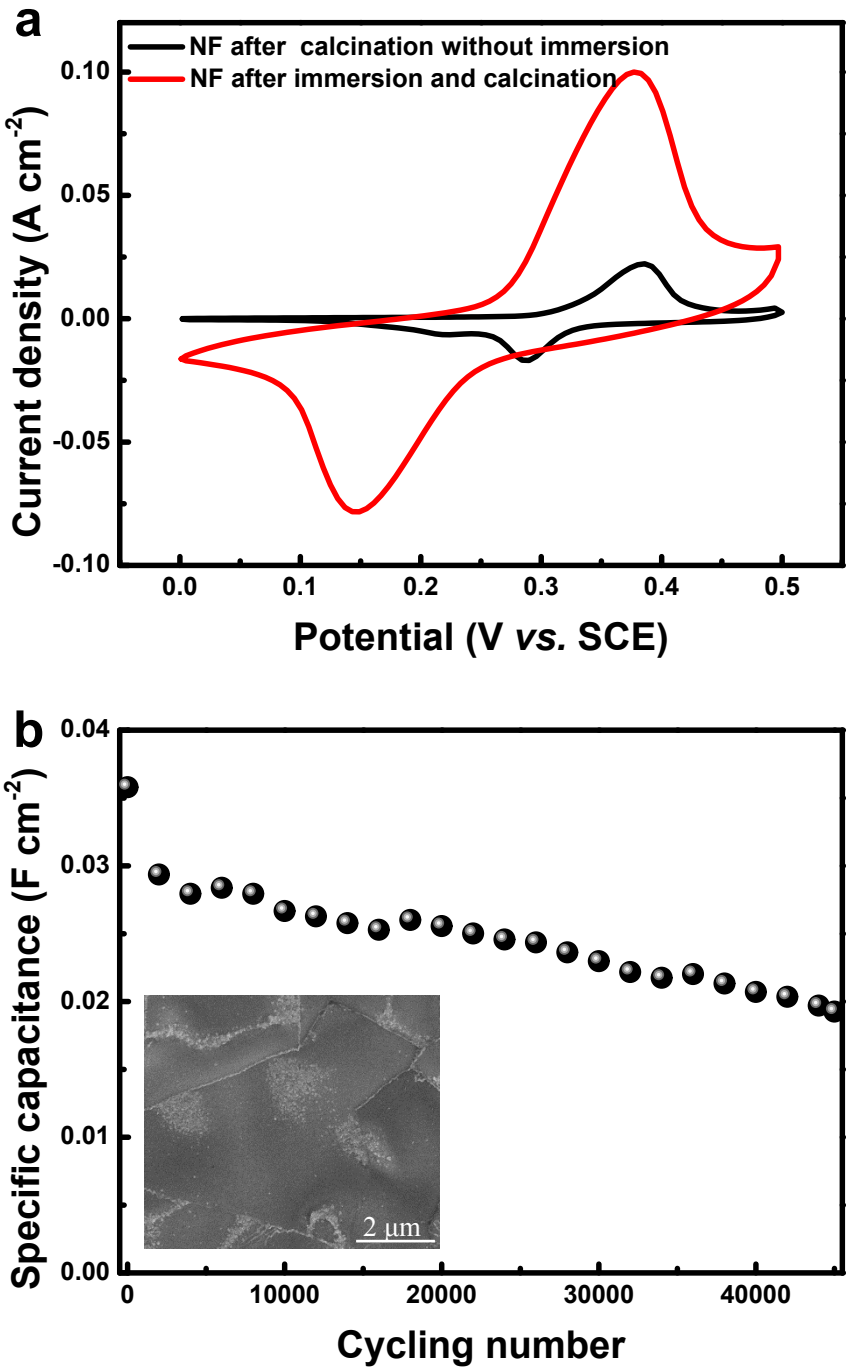

Figure S7. (a) CV curves of the nickel foam electrodes calcined at 400 ^{o}C at 100 mV s^{-1} in the 2 M KOH solution. Red curve: the Ni foam electrode after immersion and calcination; and black curve: the Ni foam electrode after calcination (without immersion). (b) Cycling stability of the calcined nickel foam electrode (without immersion treatment) measured by CV at 100 mV s^{-1} in the 2 M KOH solution. The SEM inset in (b) shows the surface morphology of the skeletons of the calcined nickel foam.

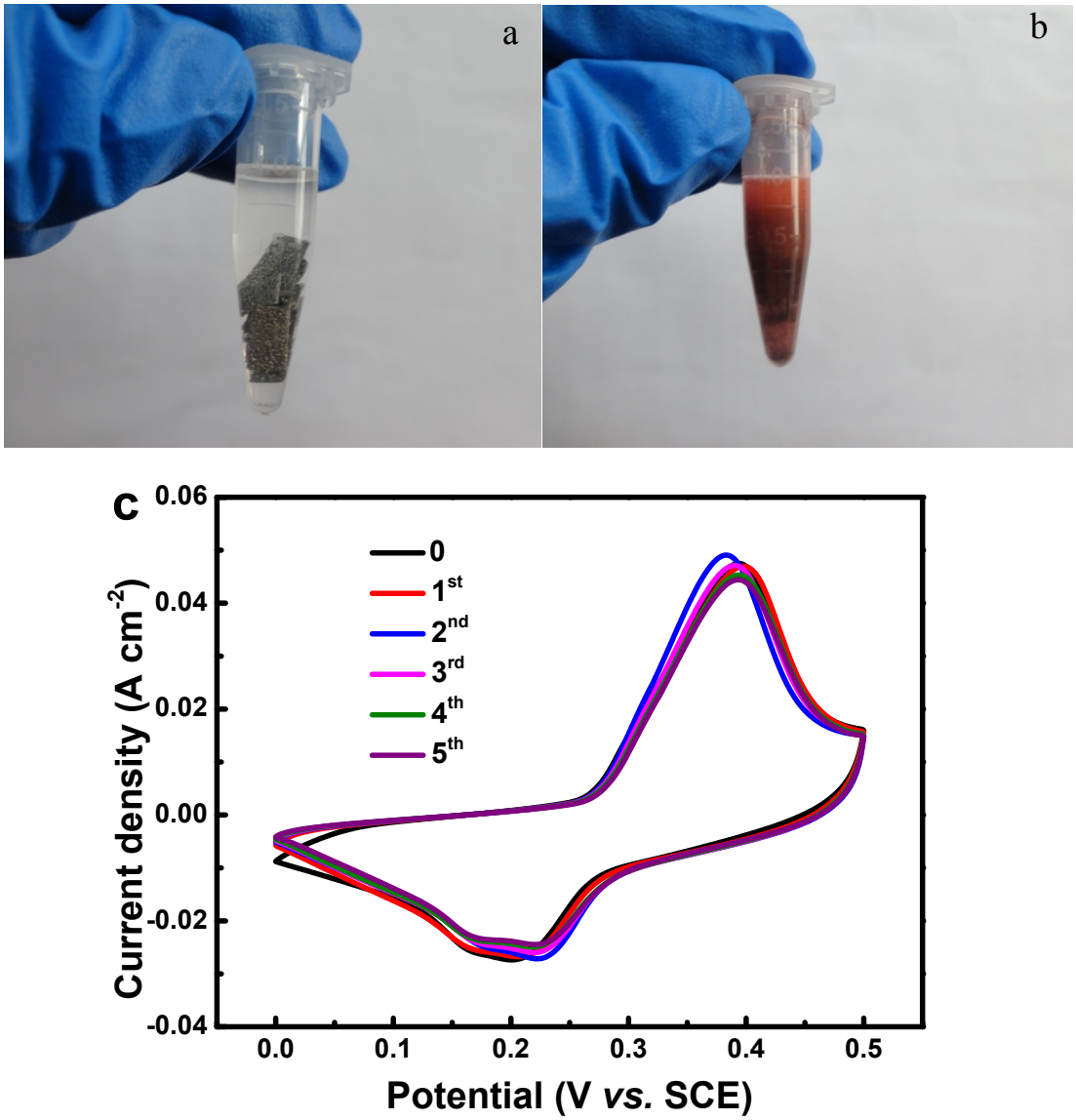

Figure S8. Photographs of (a) the present NiO hybrid electrode and (b) carbon cloth electrode with active materials after ultrasonication. (c) CV curves of the ultrathin mesoporous NiO nanosheets-anchored 3D nickel foam electrode measured in the 2 M KOH aqueous solution at 50 mV s^{-1} before and after ultrasonication treatment (the ultrosonication treatment lasted for 1 min every time).

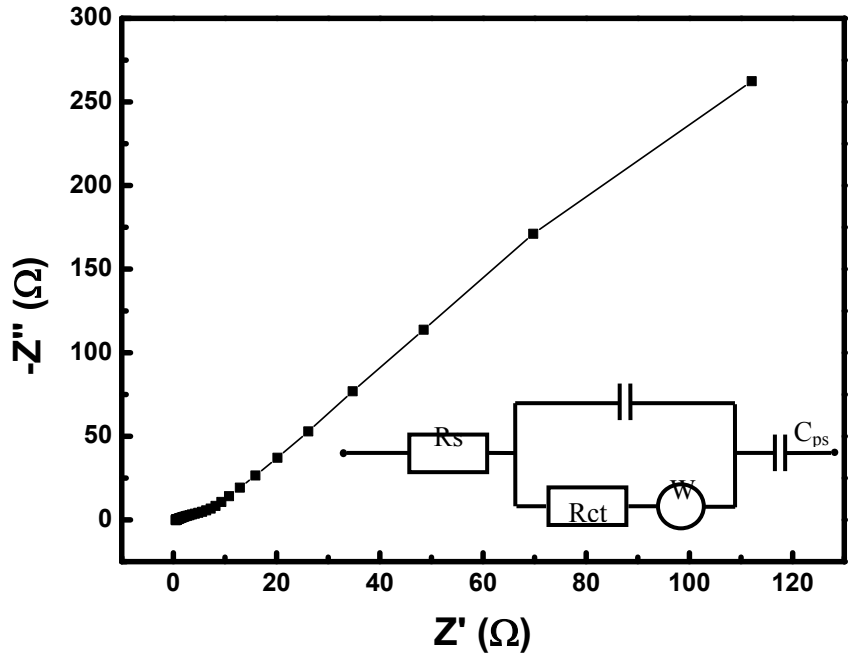

Figure S9. Nyquist diagram of the ultrathin mesoporous NiO electrode carried out at open circuit potential with a frequency ranging from 0.01 Hz to 100 kHz and the equivalent circuit diagram of different elements from the EIS analysis.

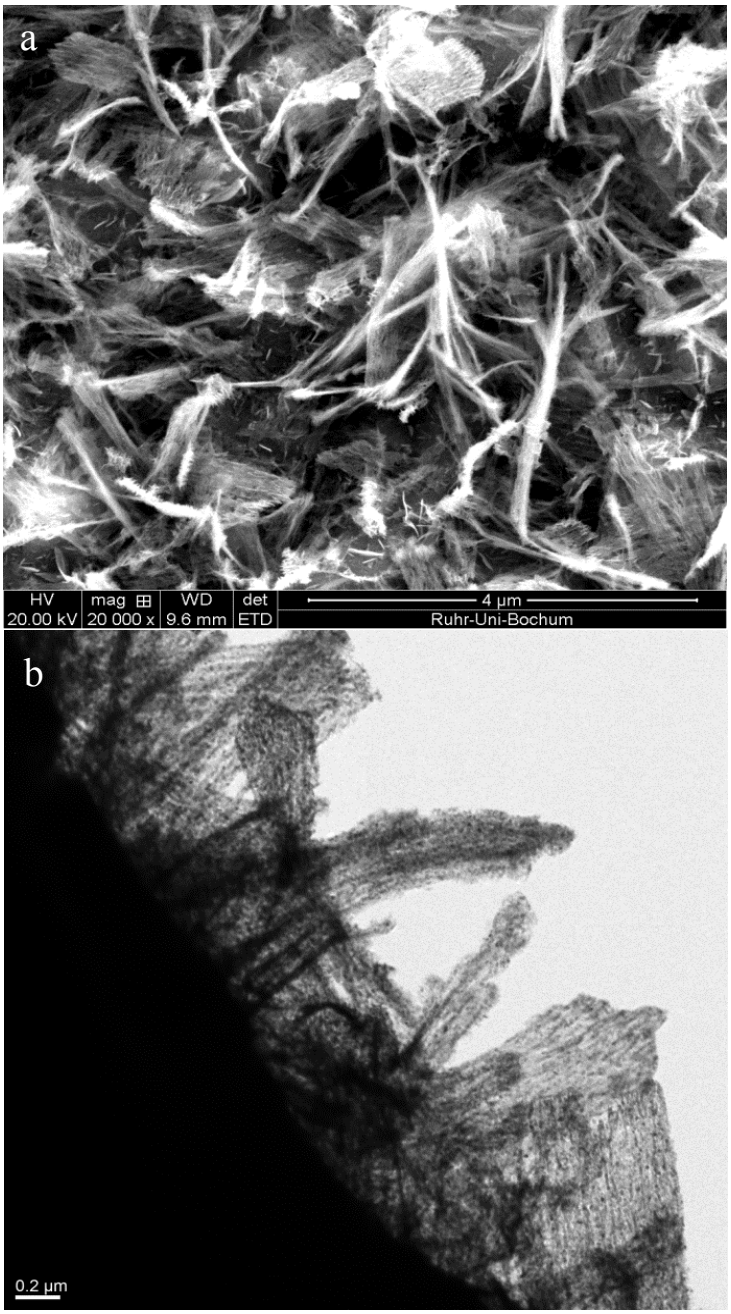

Figure S10. (a) SEM and (b) TEM images of Co_3O_4 nanosheets supported on 3D nickel foam, which were synthesized by immersing the electroplated cobalt-decorated nickel foam in the oxalic acid ethanol solution combined with subsequent calcination at 400 °C. The images show that the present strategy (immersion in combination with subsequent calcination) could be extended to fabricate other transition metal oxides electrodes with desirable nanostructures.

Table S1 Summary of electrochemical performance of NiO-based electrodes.

Materials	Specific capacitance	Capacitive retention (%)/ cycles	Ref.
Multishelled NiO hollow nanospheres	612.5 F g^{-1} (0.5 A g^{-1})	90.1%/1000	11
Hierarchical porous NiO nanotube arrays	675 F g^{-1} (2 A g^{-1})	93.2%/10000	57
Nanosheet-assembled NiO microstructures	989 F g^{-1} (3 mV s^{-1})	97%/1000	58
NiO/MWCNTs nanohybrid thin films	1727 F g^{-1} (5 mA cm^{-1})	91%/2000	59
Nickel oxide nanoflakes on 3D graphene	1829 F g^{-1} (3 A g^{-1})	85%/5000	60
NiO nanorod arrays on Ni foam	2018 F g^{-1} (2.27 A g^{-1})	92%/500	61
Homogeneous NiO nanoparticles on Ni foam	2558 F g^{-1} (2 A g^{-1})	74%/1000	62
NiO nanosheets on Ni foam	**2504.3 F g^{-1} (13.4 A g^{-1})**	**103.7%/45000**	**Present work**